

Rational synthesis, crystal structure, and sensing and adsorption properties of luminescent metal-organic frameworks

Chuanbin Fan^a, Ziao Zong^a, Xiangmin Meng^b, Xia zhang^a, Xiaoyin Zhang^a, Dongmei Zhang^a,
Cungang Xu^a, Hu Wang^a, Yuhua Fan^{a*}

- a. Key Laboratory of Marine Chemistry Theory and Technology, Ministry of Education, College of Chemistry and Chemical Engineering, Ocean University of China, Qingdao, Shandong 266100, P.R. China
- b. Shandong Provincial Key Laboratory of Biochemical Engineering, Qingdao University Science and Technology, Qingdao, Shandong 266042, P.R. China

Experimental section

Materials and physical measurements All reagents and solvents were purchased from Jinan Henghua Sci. & Tec. Co. Ltd., and were used without further purification. Elemental analysis (C, H, and N) was performed in a model 2400 Perkin-Elmer analyzer (EDX). Thermogravimetric (TG) analysis was performed on a Perkin-Elmer TG-7 thermogravimetric analyzer under nitrogen conditions from 30 to 900 °C with a heating rate of 10 °C·min⁻¹. Infrared spectra were recorded with KBr pellets on the Nicolet 170SX spectrometer in the 4000-400 cm⁻¹ region. The X-ray powder diffraction (XRPD) was collected using a PANalytical X’Pert Pro diffractometer with Cu-Kα radiation. Topological analysis was performed and confirmed by the Topos program and the Systre software.¹

X-ray crystallography Single crystals of the MOFs **1–5** with suitable dimensions were chosen under an optical microscope and fast coated with high vacuum grease (Dow Corning Corporation) before being mounted on glass fiber for data collection. X-ray crystallography data for **1–5** was collected on a Bruker Apex Smart CCD diffractometer at 173 K with graphite-monochromatized *Mo-Kα* radiation ($\lambda = 0.71073 \text{ \AA}$) by using the ω -2θ scan mode. The structure was saved by direct methods using *SHELXS-97*.² The non-hydrogen atoms were defined by the Fourier synthesis method.

Thermal and positional parameters were refined by the full matrix least-squares method (on F^2) to convergence.³ We employed PLATON/SQUEEZE to calculate the diffraction contribution of the solvent molecules and, thereby, to produce a set of solvent-free diffraction intensities.⁴ Hydrogen atoms were placed at calculated positions and included as riding atoms with isotropic displacement parameters 1.2-1.5 times U_{eq} of the attached C atoms. All structures were investigated by the Addsym subroutine of PLATON⁵ to assure that no additional symmetry could be applied to the models. Selected bond lengths and angles for **1-5** are listed in [Table S1](#). CCDC numbers for **1-5** are 1874268-1874272.

Table S1 Selected bond lengths (\AA) and angles ($^\circ$) for MOFs **1-5**

Complex 1			
Cd1—O8	2.405 (3)	Cd2—O4 ⁱⁱ	2.313 (3)
Cd1—O8 ⁱ	2.405 (3)	Cd2—O6	2.622 (3)
Cd1—O9	2.353 (3)	Cd2—O7	2.231 (3)
Cd1—O9 ⁱ	2.353 (3)	Cd2—O10 ⁱⁱ	2.572 (3)
Cd1—N4 ⁱ	2.233 (4)	Cd2—O14	2.345 (3)
Cd1—N4	2.233 (4)	Cd2—N2	2.217 (4)
Cd3—O1	2.296 (3)	Cd4—O3 ^{vi}	2.255 (3)
Cd3—O1 ⁱⁱⁱ	2.296 (3)	Cd4—O12 ^{vii}	2.189 (3)
Cd3—O10 ^{iv}	2.296 (3)	Cd4—O13 ^{viii}	2.352 (4)
Cd3—O10 ^v	2.296 (3)	Cd4—O15 ^{viii}	2.328 (4)
Cd3—O11	2.320 (3)	Cd4—O16	2.186 (3)
Cd3—O11 ⁱⁱⁱ	2.320 (3)	O3—Cd4 ^{vi}	2.255 (3)
O4—Cd2 ^{ix}	2.313 (3)	O10—Cd2 ^{ix}	2.572 (3)
O12—Cd4 ^{iv}	2.189 (3)	O10—Cd3 ^{vii}	2.296 (3)
O13—Cd4 ^x	2.352 (4)	O15—Cd4 ^x	2.328 (4)
O8 ⁱ —Cd1—O8	180.0	N4—Cd1—O8 ⁱ	92.80 (13)
O9—Cd1—O8 ⁱ	101.02 (11)	N4—Cd1—O8	87.20 (13)
O9—Cd1—O8	78.98 (11)	N4 ⁱ —Cd1—O8	92.80 (13)
O9 ⁱ —Cd1—O8	101.02 (11)	N4 ⁱ —Cd1—O8 ⁱ	87.20 (13)
O9 ⁱ —Cd1—O8 ⁱ	78.98 (11)	N4 ⁱ —Cd1—O9 ⁱ	93.05 (13)
O9—Cd1—O9 ⁱ	180.00 (17)	N4 ⁱ —Cd1—O9	86.95 (14)
N4—Cd1—O9	93.05 (13)	O4 ⁱⁱ —Cd2—C3	119.86 (13)

N4—Cd1—O9 ⁱ	86.95 (14)	O6—Cd2—C3	26.54 (12)
N4—Cd1—N4 ⁱ	180.00 (16)	O7—Cd2—O4 ⁱⁱ	94.11 (12)
O4 ⁱⁱ —Cd2—O6	146.12 (11)	O7—Cd2—O6	53.15 (11)
O4 ⁱⁱ —Cd2—O10 ⁱⁱ	52.84 (11)	O7—Cd2—O10 ⁱⁱ	130.84 (12)
O4 ⁱⁱ —Cd2—O14	124.96 (12)	O7—Cd2—O14	98.61 (13)
O7—Cd2—C3	26.93 (13)	N2—Cd2—O4 ⁱⁱ	110.50 (13)
O10 ⁱⁱ —Cd2—O6	154.21 (11)	N2—Cd2—O6	91.93 (13)
O10 ⁱⁱ —Cd2—C3	152.90 (13)	N2—Cd2—O7	135.43 (13)
O14—Cd2—O6	74.52 (12)	N2—Cd2—O10 ⁱⁱ	93.00 (13)
O14—Cd2—O10 ⁱⁱ	79.77 (11)	N2—Cd2—O14	96.67 (13)
O14—Cd2—C3	88.81 (13)	N2—Cd2—C3	112.82 (14)
O1—Cd3—O1 ⁱⁱⁱ	180.0	O1—Cd3—C30	29.07 (13)
O1 ⁱⁱⁱ —Cd3—O11 ⁱⁱⁱ	57.21 (11)	O1—Cd3—C30 ⁱⁱⁱ	150.93 (13)
O1—Cd3—O11 ⁱⁱⁱ	122.80 (11)	O1 ⁱⁱⁱ —Cd3—C30	150.93 (13)
O1 ⁱⁱⁱ —Cd3—O11	122.79 (11)	O10 ^v —Cd3—O1	91.45 (12)
O1—Cd3—O11	57.21 (11)	O10 ^v —Cd3—O1 ⁱⁱⁱ	88.55 (12)
O1 ⁱⁱⁱ —Cd3—C30 ⁱⁱⁱ	29.07 (13)	O10 ^{iv} —Cd3—O1 ⁱⁱⁱ	91.45 (12)
O10 ^{iv} —Cd3—O1	88.55 (12)	O10 ^{iv} —Cd3—C30	88.38 (13)
O10 ^v —Cd3—O10 ^{iv}	180.00 (17)	O10 ^v —Cd3—C30 ⁱⁱⁱ	88.38 (13)
O10 ^{iv} —Cd3—O11 ⁱⁱⁱ	90.59 (12)	O10 ^{iv} —Cd3—C30 ⁱⁱⁱ	91.62 (13)
O10 ^v —Cd3—O11 ⁱⁱⁱ	89.41 (12)	O10 ^v —Cd3—C30	91.62 (13)
O10 ^{iv} —Cd3—O11	89.41 (12)	O11—Cd3—O11 ⁱⁱⁱ	180.0
O10 ^v —Cd3—O11	90.59 (12)	O11—Cd3—C30	28.14 (13)
O11—Cd3—C30 ⁱⁱⁱ	151.86 (13)	O3 ^{vi} —Cd4—C24 ^{viii}	126.50 (14)
O11 ⁱⁱⁱ —Cd3—C30 ⁱⁱⁱ	28.14 (13)	O12 ^{vii} —Cd4—O3 ^{vi}	102.16 (13)
O11 ⁱⁱⁱ —Cd3—C30	151.86 (13)	O12 ^{vii} —Cd4—O13 ^{viii}	92.71 (14)
C30 ⁱⁱⁱ —Cd3—C30	180.0	O12 ^{vii} —Cd4—O15 ^{viii}	115.70 (14)
O3 ^{vi} —Cd4—O13 ^{viii}	154.33 (13)	O12 ^{vii} —Cd4—C24 ^{viii}	105.86 (14)
O3 ^{vi} —Cd4—O15 ^{viii}	98.53 (13)	O13 ^{viii} —Cd4—C24 ^{viii}	27.91 (14)
O15 ^{viii} —Cd4—O13 ^{viii}	55.93 (12)	O16—Cd4—O13 ^{viii}	95.31 (15)
O15 ^{viii} —Cd4—C24 ^{viii}	28.02 (14)	O16—Cd4—O15 ^{viii}	110.30 (14)
O16—Cd4—O3 ^{vi}	91.45 (14)	O16—Cd4—C24 ^{viii}	104.31 (15)
O16—Cd4—O12 ^{vii}	128.98 (13)		

Symmetry codes: (i) $-x, -y+1, -z+1$; (ii) $x, y+1, z$; (iii) $-x+2, -y+1, -z$; (iv) $x+1, y, z$; (v) $-x+1, -y+1, -z$; (vi) $-x, -y+2, -z+1$; (vii) $x-1, y, z$; (viii) $x-1, y+1, z$; (ix) $x, y-1, z$; (x) $x+1, y-1, z$.

Complex 2			
Cd1—O6	2.257 (3)	Cd1—O2 ⁱ	2.445 (3)
Cd1—O1 ⁱ	2.380 (3)	Cd1—N4 ⁱⁱⁱ	2.288 (3)
Cd1—O7 ⁱⁱ	2.300 (3)	Cd1—N1	2.277 (3)
O1—Cd1 ^{iv}	2.380 (3)	N4—Cd1 ^v	2.288 (3)
O7—Cd1 ⁱⁱ	2.300 (3)	O2—Cd1 ^{iv}	2.445 (3)
O6—Cd1—O1 ⁱ	147.47 (10)	O1 ⁱ —Cd1—O2 ⁱ	54.09 (9)
O6—Cd1—O7 ⁱⁱ	124.52 (11)	O7 ⁱⁱ —Cd1—O1 ⁱ	87.98 (10)
O6—Cd1—O2 ⁱ	93.46 (10)	O7 ⁱⁱ —Cd1—O2 ⁱ	141.49 (10)
O6—Cd1—N4 ⁱⁱⁱ	95.24 (11)	N4 ⁱⁱⁱ —Cd1—O1 ⁱ	85.10 (11)
O6—Cd1—N1	86.11 (11)	N4 ⁱⁱⁱ —Cd1—O7 ⁱⁱ	90.22 (12)
N4 ⁱⁱⁱ —Cd1—O2 ⁱ	92.52 (12)	N1—Cd1—O2 ⁱ	90.41 (11)
N1—Cd1—O1 ⁱ	95.40 (11)	N1—Cd1—N4 ⁱⁱⁱ	176.69 (13)
N1—Cd1—O7 ⁱⁱ	86.53 (11)		

Symmetry codes: (i) $x, -y, z-1/2$; (ii) $-x+2, -y, -z+1$; (iii) $x+1, y-1, z$; (iv) $x, -y, z+1/2$; (v) $x-1, y+1, z$.

Complex 3			
Cd2—O4 ⁱ	2.2538 (18)	Cd1—O1	2.2459 (18)
Cd2—O4 ⁱⁱ	2.2539 (17)	Cd1—O3 ^{iv}	2.3317 (17)
Cd2—O5 ⁱⁱⁱ	2.6340 (18)	Cd1—O6 ^v	2.5136 (16)
Cd2—O5	2.6339 (18)	Cd1—O8	2.4149 (18)
Cd2—O6 ⁱⁱⁱ	2.2707 (15)	Cd1—N1	2.226 (2)
Cd2—O6	2.2707 (15)	Cd1—N4 ^{vi}	2.225 (2)
O3—Cd1 ^{iv}	2.3316 (17)	O6—Cd1 ^v	2.5135 (16)
O4—Cd2 ^{vii}	2.2538 (17)	N4—Cd1 ^{viii}	2.225 (2)
O4 ⁱ —Cd2—O4 ⁱⁱ	108.88 (10)	O4 ⁱⁱ —Cd2—O6 ⁱⁱⁱ	114.11 (6)
O4 ⁱⁱ —Cd2—O5	85.97 (7)	O5—Cd2—O5 ⁱⁱⁱ	81.30 (9)
O4 ⁱ —Cd2—O5	162.32 (6)	O6—Cd2—O5 ⁱⁱⁱ	84.71 (6)
O4 ⁱⁱ —Cd2—O5 ⁱⁱⁱ	162.32 (7)	O6 ⁱⁱⁱ —Cd2—O5	84.71 (6)
O4 ⁱ —Cd2—O5 ⁱⁱⁱ	85.97 (7)	O6 ⁱⁱⁱ —Cd2—O5 ⁱⁱⁱ	52.68 (5)
O4 ⁱ —Cd2—O6 ⁱⁱⁱ	97.29 (6)	O6—Cd2—O5	52.67 (5)
O4 ⁱ —Cd2—O6	114.11 (6)	O6 ⁱⁱⁱ —Cd2—O6	125.18 (8)
O4 ⁱⁱ —Cd2—O6	97.29 (6)	O1—Cd1—O3 ^{iv}	86.63 (7)

O1—Cd1—O6 ^v	161.88 (6)	N1—Cd1—O3 ^{iv}	90.36 (7)
O1—Cd1—O8	82.15 (7)	N1—Cd1—O6 ^v	82.30 (7)
O3 ^{iv} —Cd1—O6 ^v	75.44 (6)	N1—Cd1—O8	87.13 (7)
O3 ^{iv} —Cd1—O8	167.83 (6)	N4 ^{vi} —Cd1—O1	95.75 (8)
O8—Cd1—O6 ^v	115.94 (6)	N4 ^{vi} —Cd1—O3 ^{iv}	95.49 (7)
N1—Cd1—O1	100.64 (8)	N4 ^{vi} —Cd1—O6 ^v	83.64 (7)
N4 ^{vi} —Cd1—O8	90.31 (7)	N4 ^{vi} —Cd1—N1	162.89 (8)

Symmetry codes: (i) $x+1/2, y+1/2, z$; (ii) $-x+3/2, y+1/2, -z+3/2$; (iii) $-x+2, y, -z+3/2$; (iv) $-x+1, -y+1, -z+1$; (v) $-x+3/2, -y+3/2, -z+1$; (vi) $x+1, y, z$; (vii) $x-1/2, y-1/2, z$; (viii) $x-1, y, z$.

Complex 4			
Cd1—O1	2.185 (4)	O6—Cd1 ⁱⁱⁱ	2.316 (4)
Cd1—O6 ⁱ	2.316 (4)	O7—Cd1 ⁱⁱⁱ	2.416 (4)
Cd1—O7 ⁱ	2.416 (4)	N4—Cd1 ^{iv}	2.249 (4)
Cd1—N1	2.230 (4)	Cd1—N4 ⁱⁱ	2.249 (4)
O1—Cd1—O6 ⁱ	123.68 (16)	O6 ⁱ —Cd1—C14 ⁱ	27.76 (14)
O1—Cd1—O7 ⁱ	94.71 (14)	O7 ⁱ —Cd1—C14 ⁱ	27.50 (13)
O1—Cd1—N1	123.88 (16)	N1—Cd1—O6 ⁱ	87.16 (15)
O1—Cd1—N4 ⁱⁱ	100.61 (15)	N1—Cd1—O7 ⁱ	138.13 (15)
O1—Cd1—C14 ⁱ	111.65 (16)	N1—Cd1—N4 ⁱⁱ	98.28 (16)
O6 ⁱ —Cd1—O7 ⁱ	55.24 (13)	N1—Cd1—C14 ⁱ	112.92 (17)
N4 ⁱⁱ —Cd1—O6 ⁱ	121.85 (15)	N4 ⁱⁱ —Cd1—C14 ⁱ	105.86 (15)
N4 ⁱⁱ —Cd1—O7 ⁱ	88.72 (14)		

Symmetry codes: (i) $x+1, y, z$; (ii) $-x+3/2, -y+1, z+1/2$; (iii) $x-1, y, z$; (iv) $-x+3/2, -y+1, z-1/2$.

Complex 5			
Cd1—O6	2.519 (2)	Cd1—N1	2.259 (2)
Cd1—O4 ⁱ	2.411 (2)	Cd2—O2	2.248 (2)
Cd1—O1	2.342 (2)	Cd2—O2 ⁱⁱⁱ	2.248 (2)
Cd1—O3 ⁱ	2.461 (2)	Cd2—O5	2.255 (2)
Cd1—O9 ⁱⁱ	2.572 (2)	Cd2—O5 ⁱⁱⁱ	2.255 (2)
Cd1—O8 ⁱⁱ	2.357 (2)	Cd2—O9 ⁱⁱ	2.259 (2)
Cd2—O9 ^{iv}	2.259 (2)	O3—Cd1 ^v	2.461 (2)
O4—Cd1 ^v	2.412 (2)	O9—Cd1 ⁱⁱ	2.572 (2)
O8—Cd1 ⁱⁱ	2.357 (2)	O9—Cd2 ^{vi}	2.259 (2)

O6—Cd1—O9 ⁱⁱ	67.96 (7)	O1—Cd1—O3 ⁱ	79.21 (7)
O4 ⁱ —Cd1—O6	82.94 (7)	O1—Cd1—O9 ⁱⁱ	90.30 (7)
O4 ⁱ —Cd1—O3 ⁱ	53.85 (7)	O1—Cd1—O8 ⁱⁱ	96.61 (8)
O4 ⁱ —Cd1—O9 ⁱⁱ	119.96 (7)	O3 ⁱ —Cd1—O6	136.30 (7)
O1—Cd1—O6	144.04 (7)	O3 ⁱ —Cd1—O9 ⁱⁱ	136.01 (7)
O1—Cd1—O4 ⁱ	132.96 (7)	O8 ⁱⁱ —Cd1—O6	92.10 (8)
O8 ⁱⁱ —Cd1—O4 ⁱ	79.18 (8)	N1—Cd1—O3 ⁱ	95.32 (8)
O8 ⁱⁱ —Cd1—O3 ⁱ	86.32 (8)	N1—Cd1—O9 ⁱⁱ	128.33 (8)
O8 ⁱⁱ —Cd1—O9 ⁱⁱ	52.31 (7)	N1—Cd1—O8 ⁱⁱ	168.17 (9)
N1—Cd1—O6	78.61 (8)	O2—Cd2—O2 ⁱⁱⁱ	180.0
N1—Cd1—O4 ⁱ	92.30 (8)	O2 ⁱⁱⁱ —Cd2—O5	82.95 (8)
N1—Cd1—O1	95.20 (8)	O2 ⁱⁱⁱ —Cd2—O5 ⁱⁱⁱ	97.05 (8)
O2—Cd2—O5 ⁱⁱⁱ	82.95 (8)	O2 ⁱⁱⁱ —Cd2—O9 ^{iv}	81.90 (8)
O2—Cd2—O5	97.05 (8)	O2—Cd2—O9 ^{iv}	98.10 (8)
O2—Cd2—O9 ⁱⁱ	81.90 (8)	O2 ⁱⁱⁱ —Cd2—O9 ⁱⁱ	98.10 (8)
O5—Cd2—O9 ⁱⁱ	90.26 (8)	O5—Cd2—O5 ⁱⁱⁱ	180.0
O5—Cd2—O9 ^{iv}	89.74 (8)	O5 ⁱⁱⁱ —Cd2—O9 ⁱⁱ	89.74 (8)
O9 ⁱⁱ —Cd2—O9 ^{iv}	180.00 (13)	O5 ⁱⁱⁱ —Cd2—O9 ^{iv}	90.26 (8)

Symmetry codes: (i) $x, y+1, z$; (ii) $-x+2, -y+1, -z+1$; (iii) $-x+1, -y+1, -z+1$; (iv) $x-1, y, z$; (v) $x, y-1, z$; (vi) $x+1, y, z$; (vii) $-x, -y+1, -z+2$.

Table S2 The coordination modes of H₃L ligand and the roles of ancillary ligands in MOFs **1–5**

Complex	Coord. modes	Ancillary ligand/role	Dihedral angles (°) of H ₃ L	Structure and topology
1	Mode III, Mode IV-1	1,3-bit/bridging	71.994° and 73.773°	3D (3, 3, 4, 4, 8, 8)-c (3.4.5) ₂ (3 ² .4 ² .5 ² .6 ⁶ .7 ⁸ .8 ⁷ .9)(3 ² .6 ³ .7)(4.6 ⁴ .8)(4 ¹⁰ .6 ¹¹ .8 ⁷)(4 ³) ₂ unprecedented net
2	Mode II	4,4'-bbibp/chelating	79.519°	3D 2-fold 4-c (6 ⁵ .8)-cds net
3	Mode V	1,4-bimb/bridging	56.079°	3D (3,8)-c (4 ² .5) ₂ (4 ⁴ .5 ⁶ .6 ¹⁰ .7 ⁵ .8 ² .9) unprecedented net
4	Mode I	4,4'-bidpe/chelating	66.337°	3D 4-c (4 ⁴ .6 ²)-sql net
5	Mode IV-2	1,1'-bbi/bridging	82.343°	3D (3,8)-c (4 ³) ₂ (4 ⁶ .6 ¹⁸ .8 ⁴)-tfz-d net

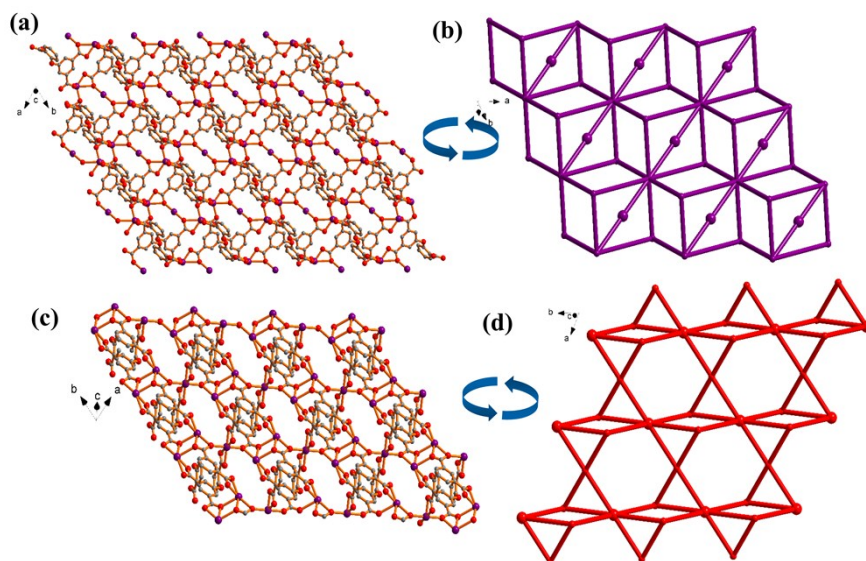


Fig. S1 (a) View of the single 2D layer of **1**; (b) with its topology structure; (c) View of the single 2D layer of **1**; (d) with its topology structure (right).

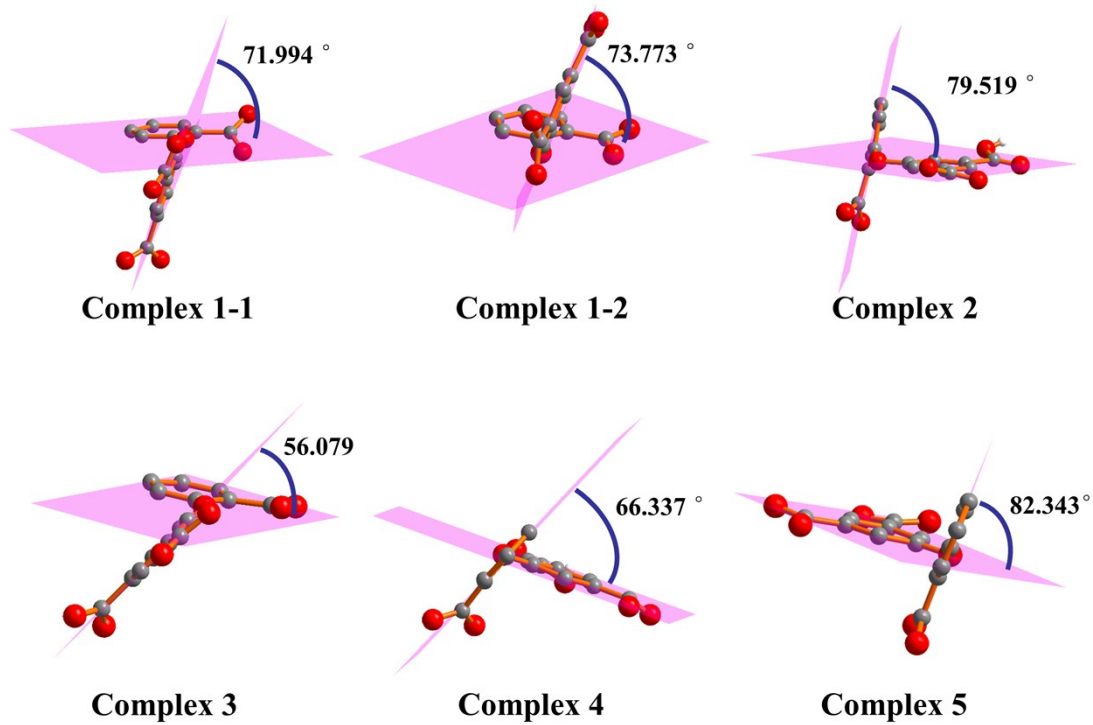


Fig. S2 The dihedral angles between the two phenyl rings in MOFs **1–5**.

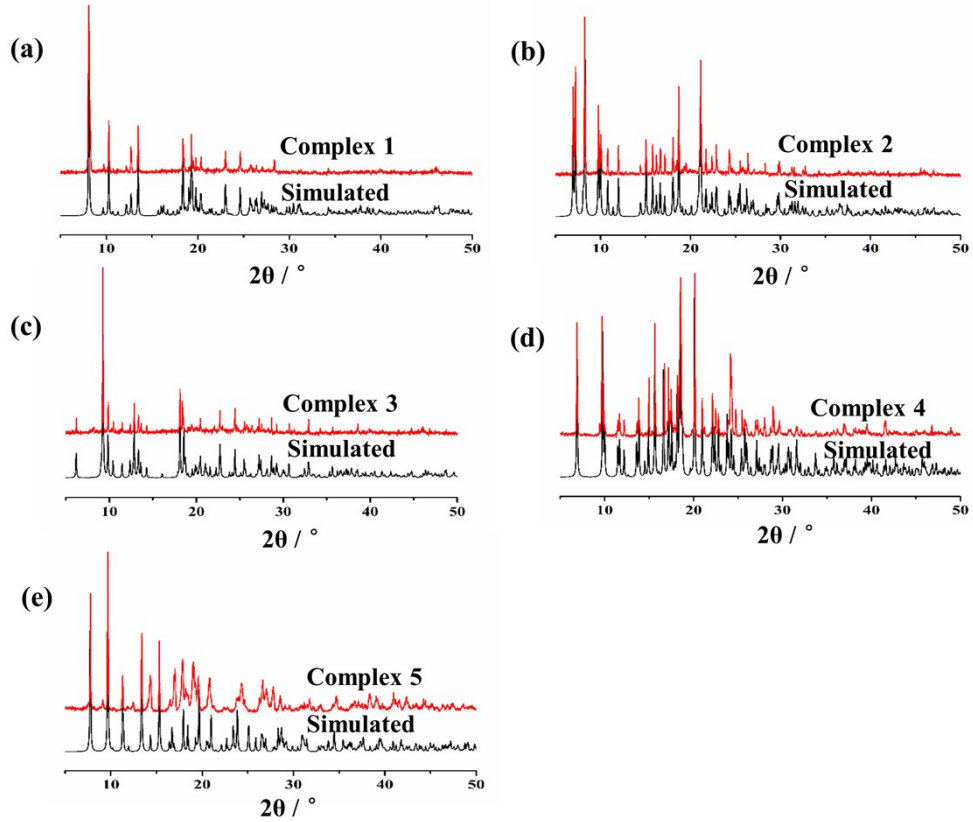


Fig. S3 The comparison of PXRD for MOFs 1–5.

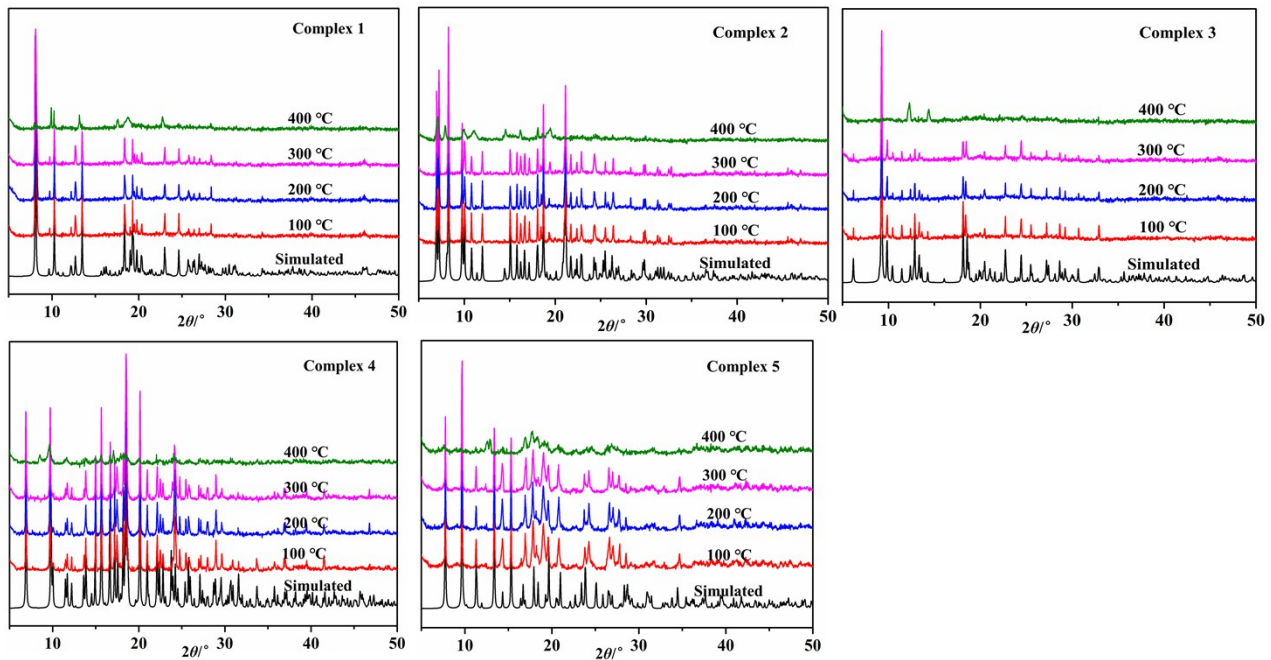


Fig. S4 Thermal stability tests for MOFs 1–5 monitored by PXRD analysis.

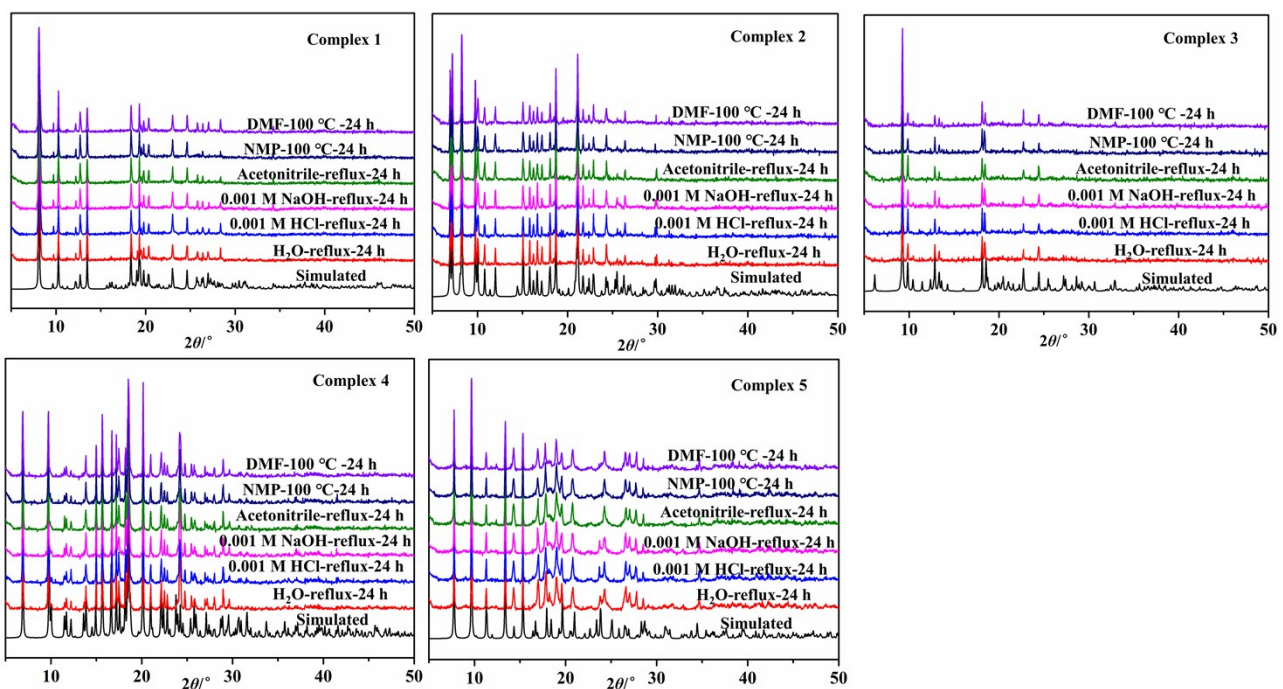


Fig. S5 Chemical stability tests for MOFs 1–5 monitored by PXRD analysis.

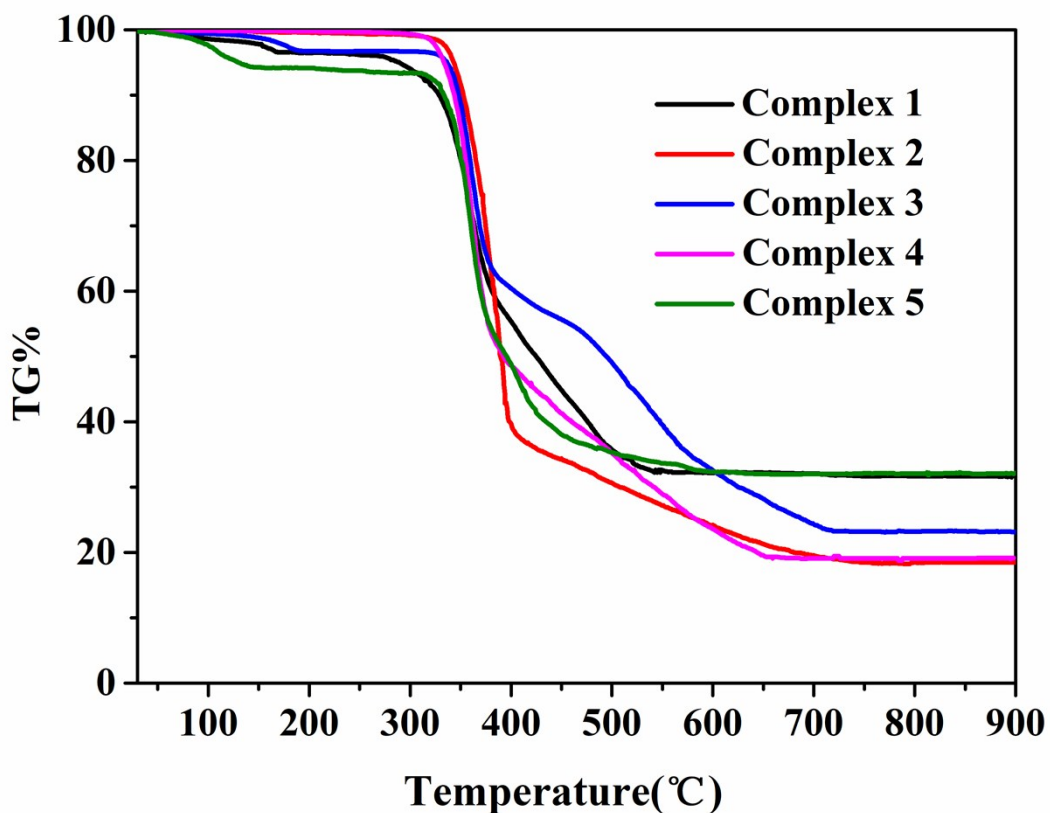


Fig. S6 The TG curves for MOFs 1–5.

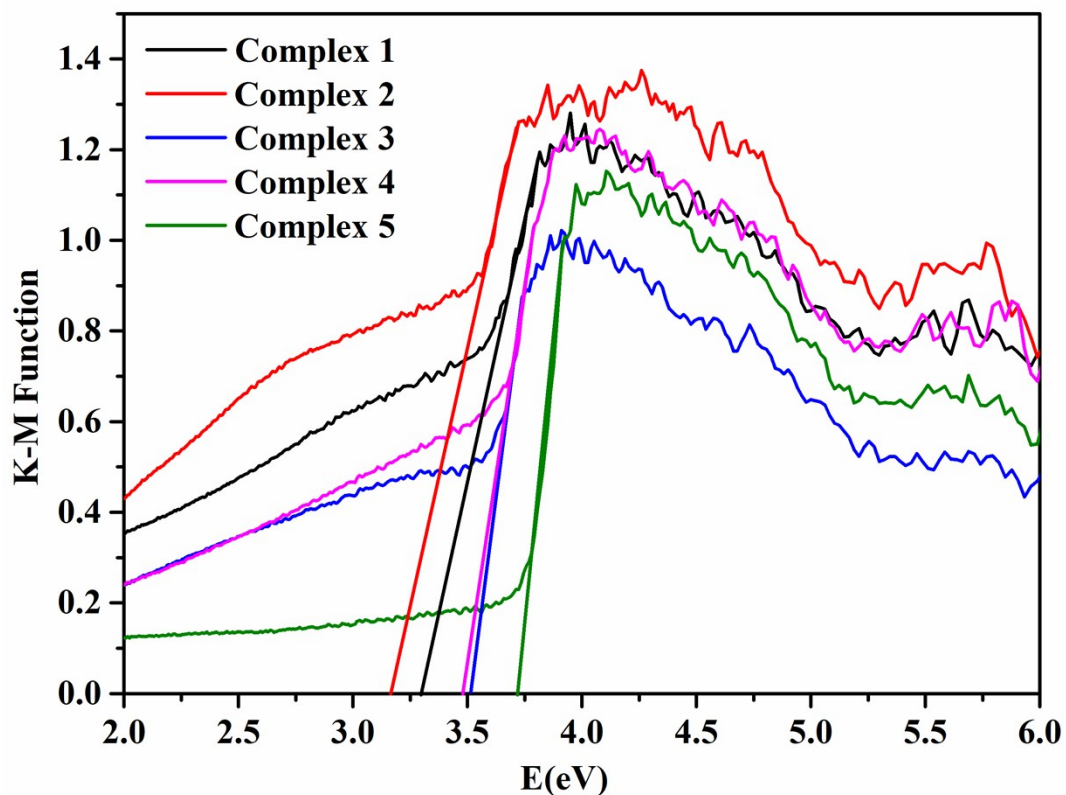


Fig. S7 Kubelka–Munk–transformed diffuse reflectance spectra of MOFs 1–5.

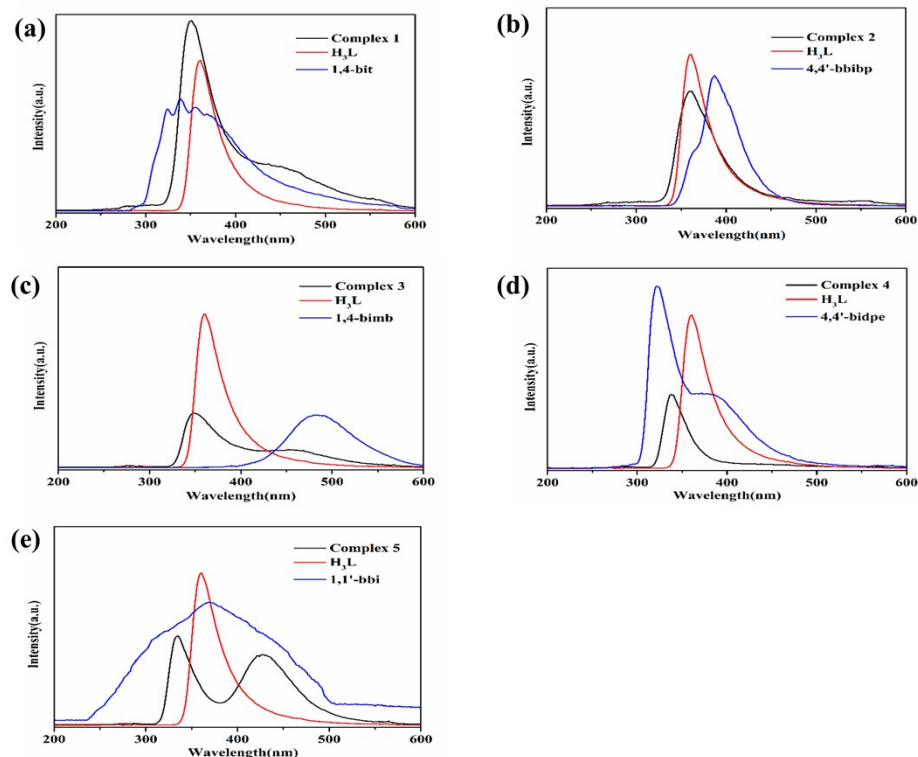


Fig. S8 (a)-(e) Photoluminescence of MOFs 1–5 at room temperature in the solid state.

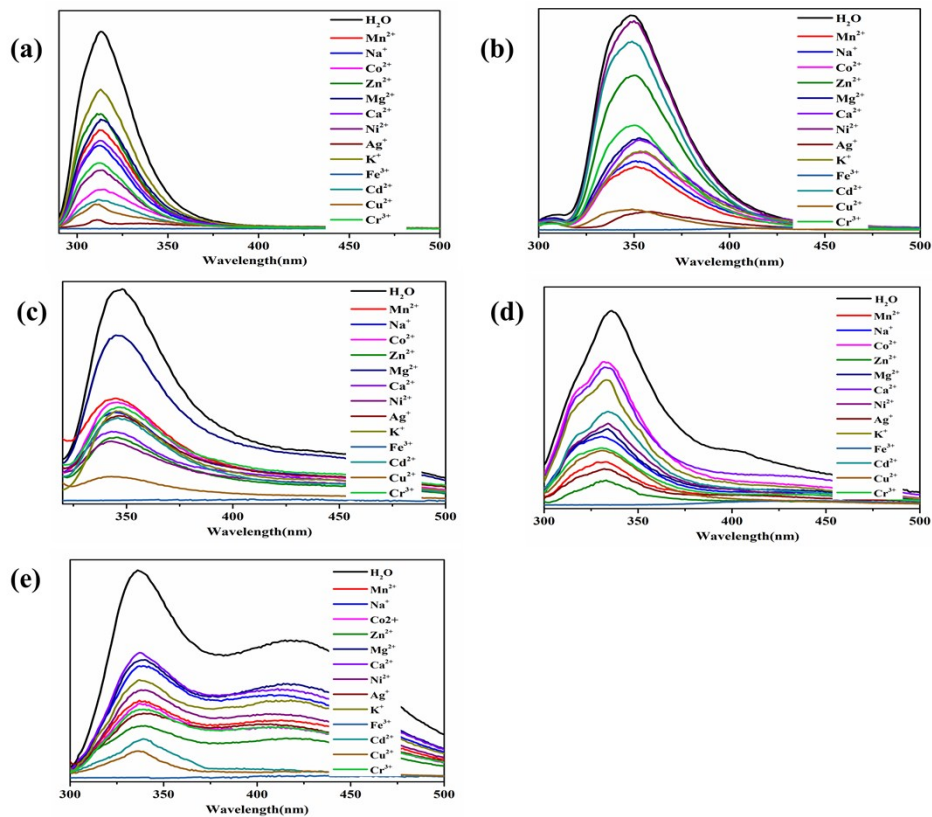


Fig. S9 (a)-(e) Photoluminescence spectra of MOFs **1–5** introduced into different metal ions dissolved in aqueous solution when excited at 279 nm for **1**, 275 nm for **2**, 279 nm for **3**, 283 nm for **4**, 280 nm for **5**.

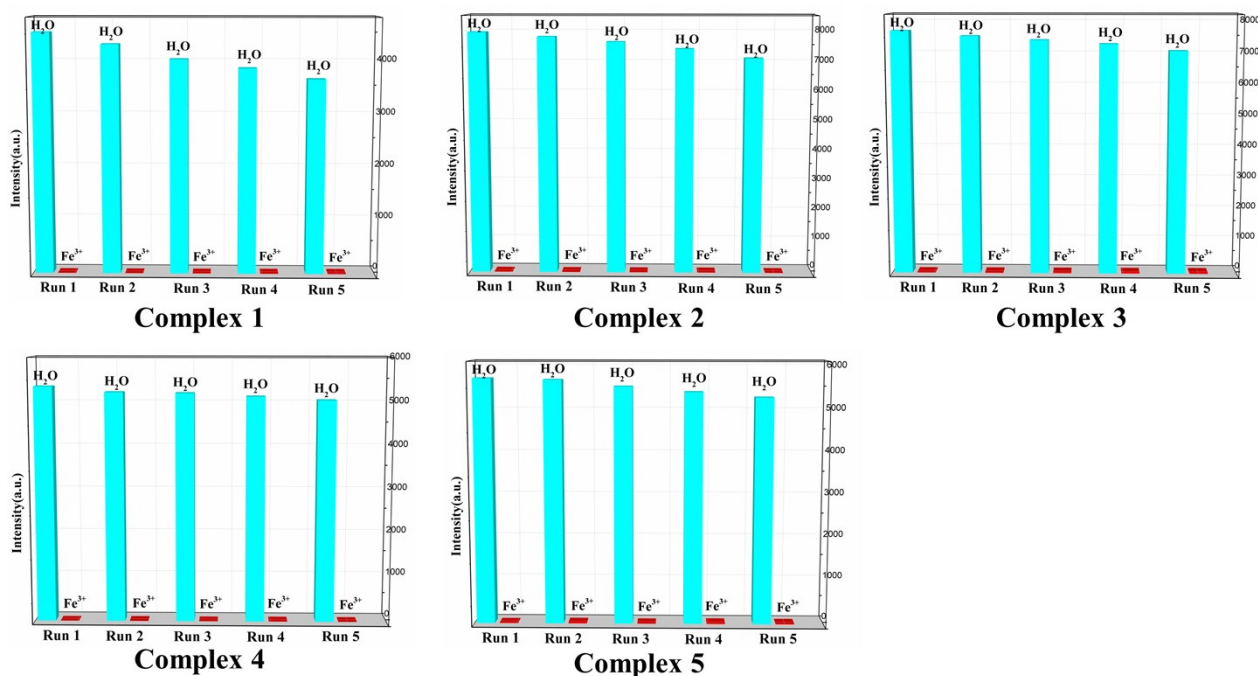


Fig. S10 The recycle performance of MOFs **1–5** for fluorescence sensing of Fe³⁺ ions.

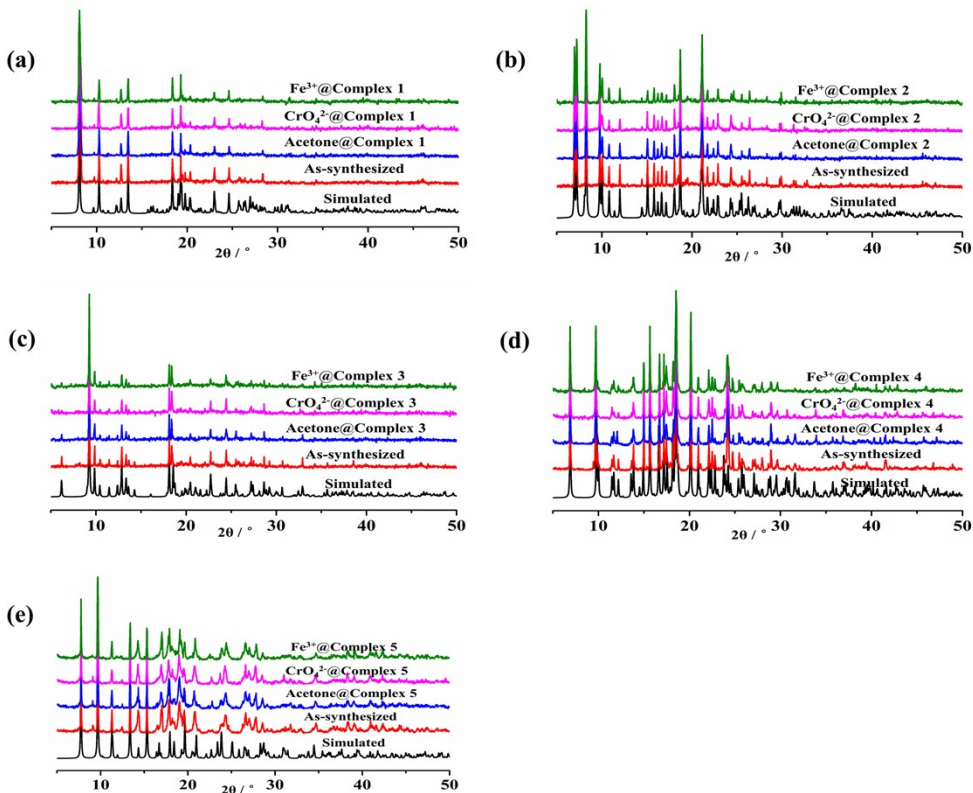


Fig. S11 (a)-(e) The PXRD pattern of MOFs **1–5** after sensing of Fe^{3+} , CrO_4^{2-} and acetone molecule.

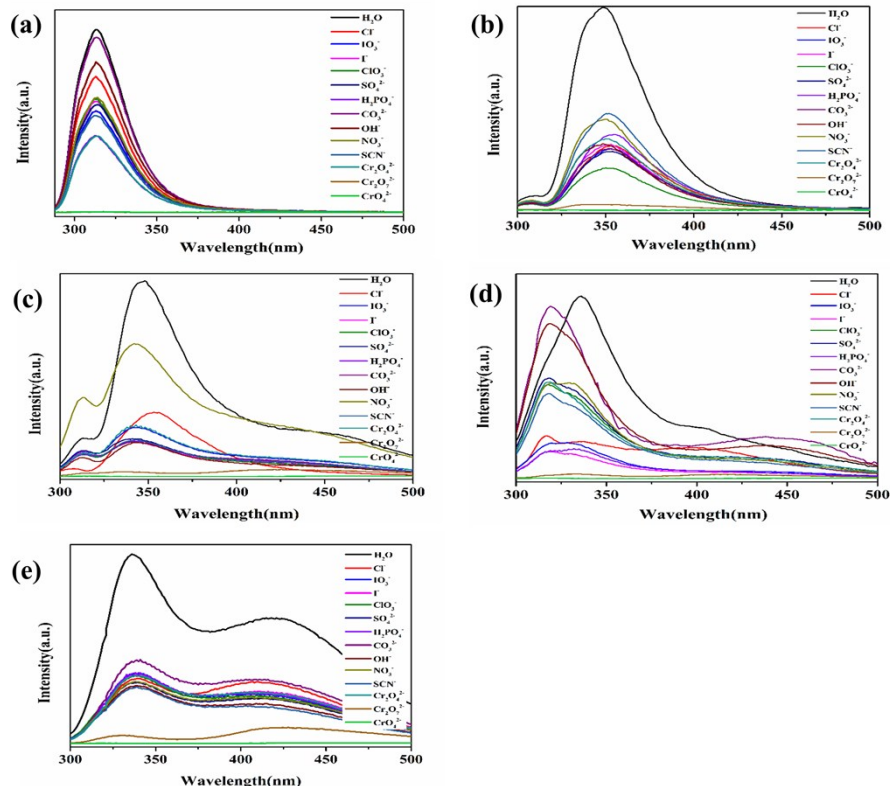


Fig. S12 (a)-(e) Photoluminescence spectra of MOFs **1–5** introduced into different anions dissolved in aqueous solution when excited at 279 nm for **1**, 275 nm for **2**, 279 nm for **3**, 283 nm for **4**, 280 nm for **5**.

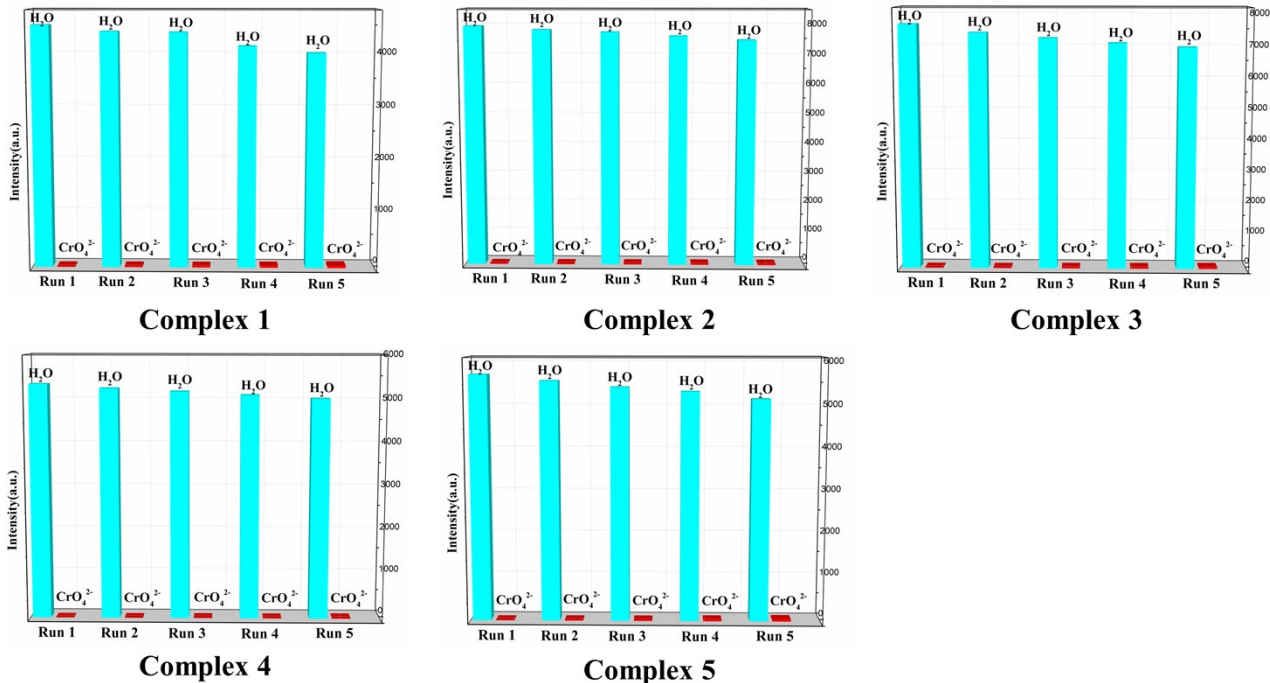


Fig. S13 The recycle performance of MOFs **1–5** for fluorescence sensing of CrO₄²⁻ anion.

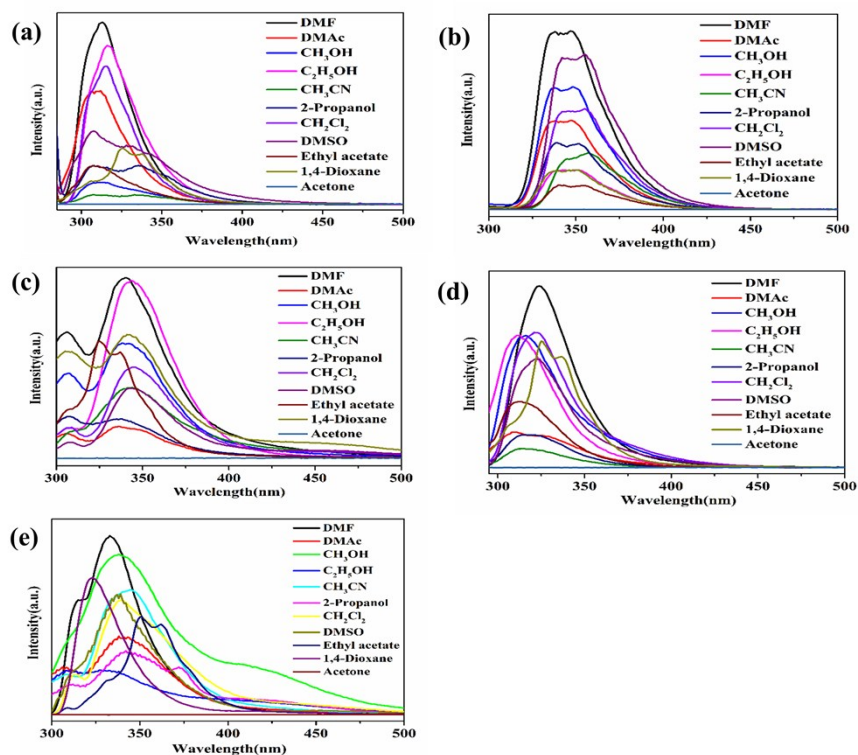


Fig. S14 (a)-(e) Photoluminescence spectra of MOFs **1–5** introduced into varied pure solvents when excited at 279 nm for **1**, 275 nm for **2**, 279 nm for **3**, 283 nm for **4**, 280 nm for **5**.

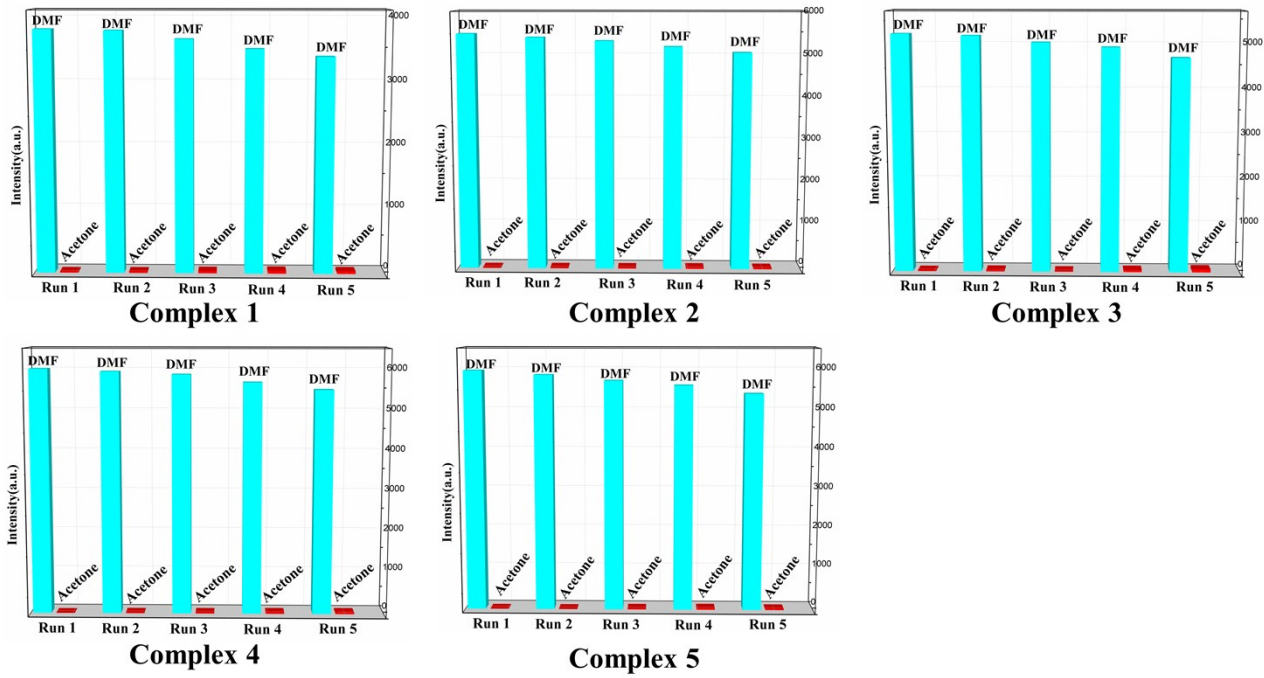


Fig. S15 The recycle performance of MOFs 1–5 for fluorescence sensing of acetone molecule.

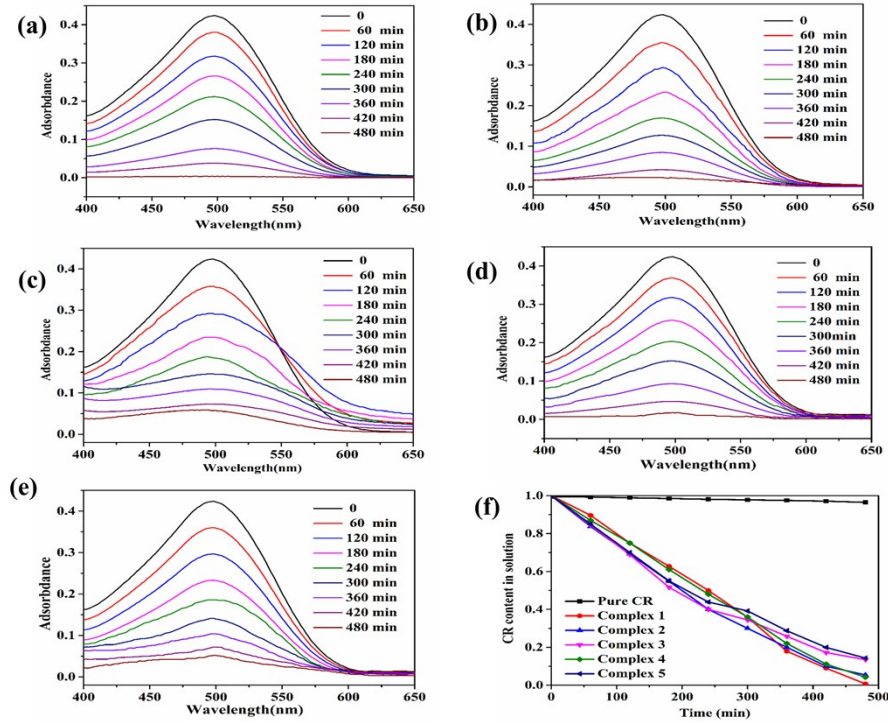


Fig. S16 (a)–(e) UV-vis spectra for the uptake of CR from aqueous solutions at various time intervals for MOFs 1–5, respectively. (f) The removal percentage (%) of CR against irradiation time (min) in the presence of MOFs 1–5, and without any catalyst during the adsorption process.

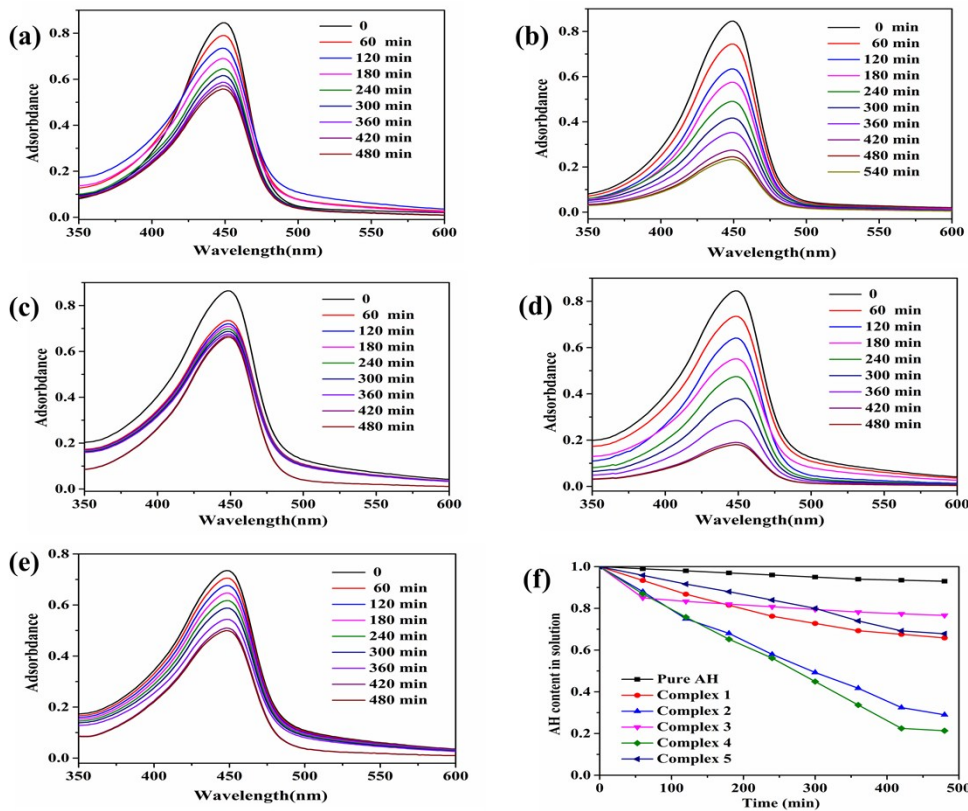


Fig. S17 (a)-(e) UV-vis spectra for the uptake of AH from aqueous solutions at various time intervals for MOFs 1–5, respectively. (f) The removal percentage (%) of AH against irradiation time (min) in the presence of MOFs 1–5, and without any catalyst during the adsorption process.

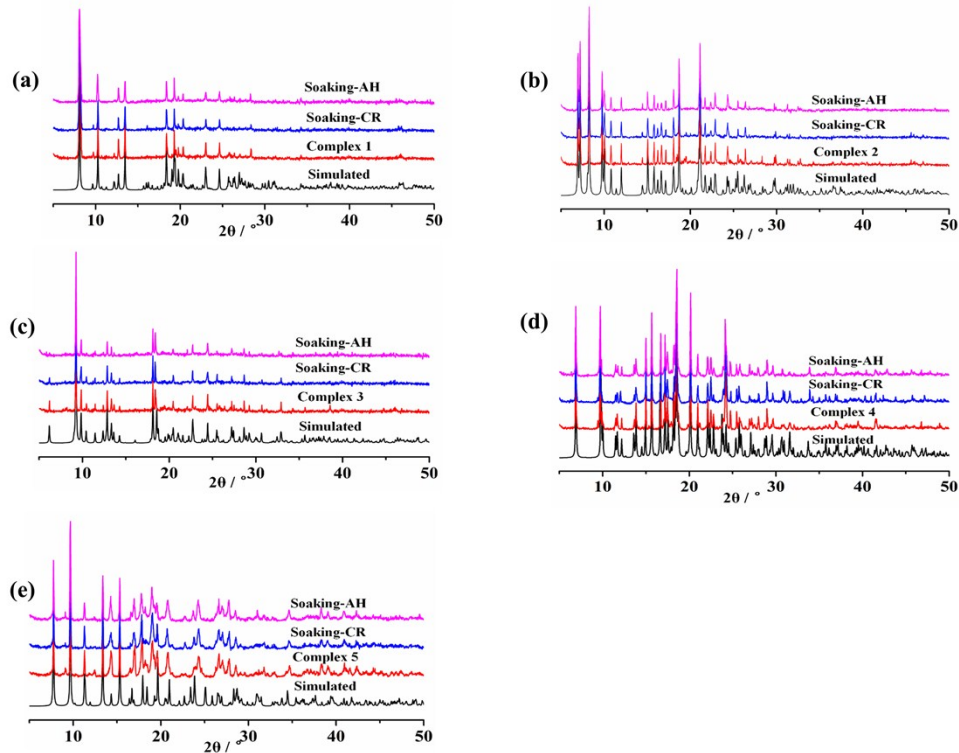


Fig. S18 (a)-(e) Comparison of PXRD for MOFs 1–5 after dye adsorption.

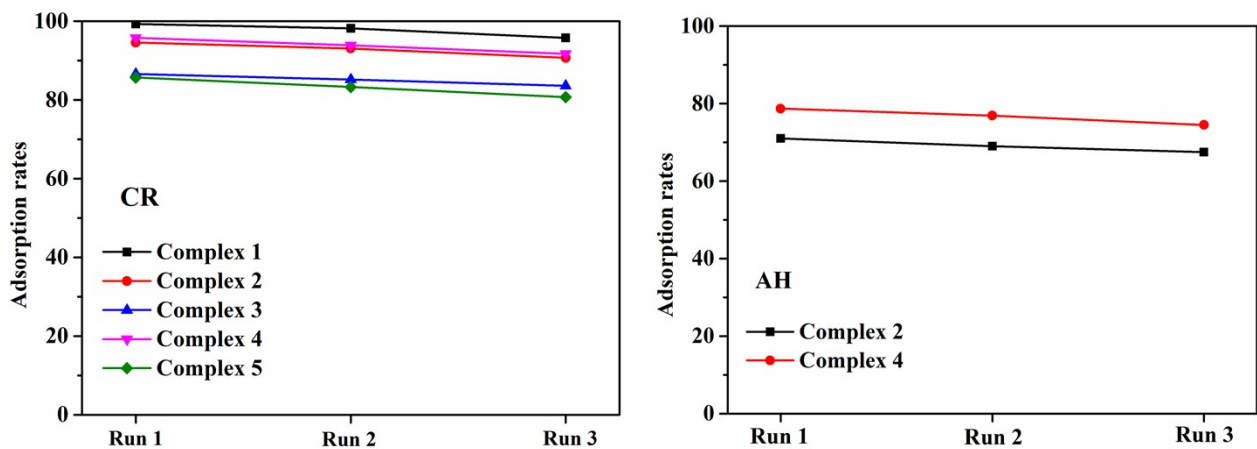


Fig. S19 The recycle adsorption performance of MOFs 1–5 for CR and MOFs 2 and 4 for AH.

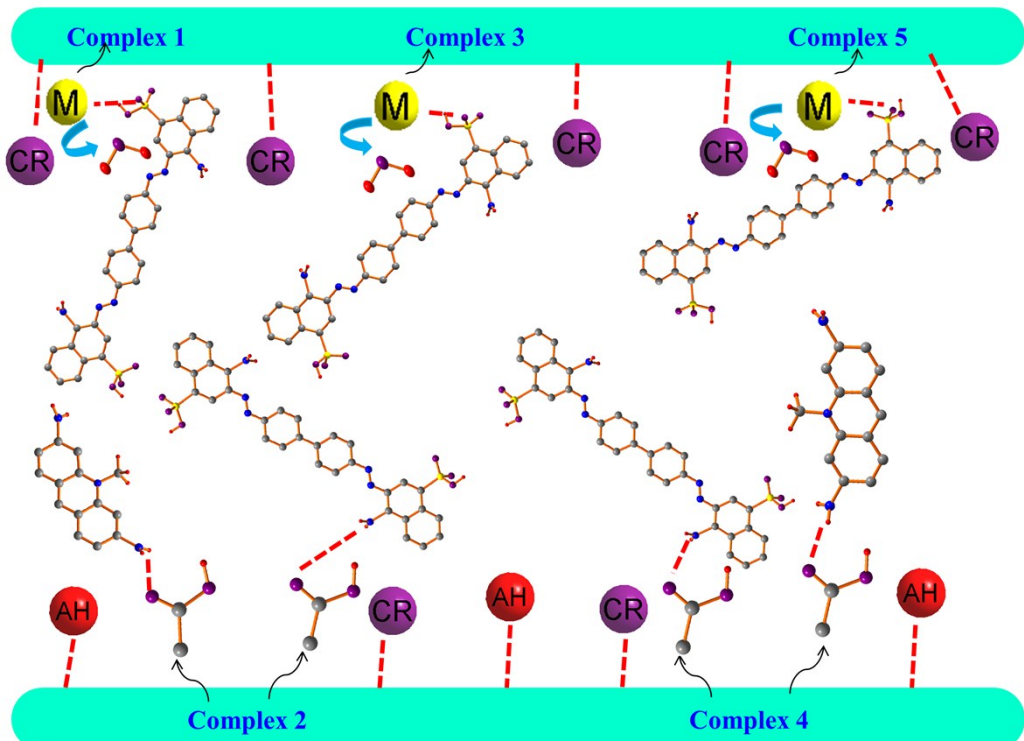


Fig. S20 The possible mechanism between two organic dyes and MOFs 1–5.

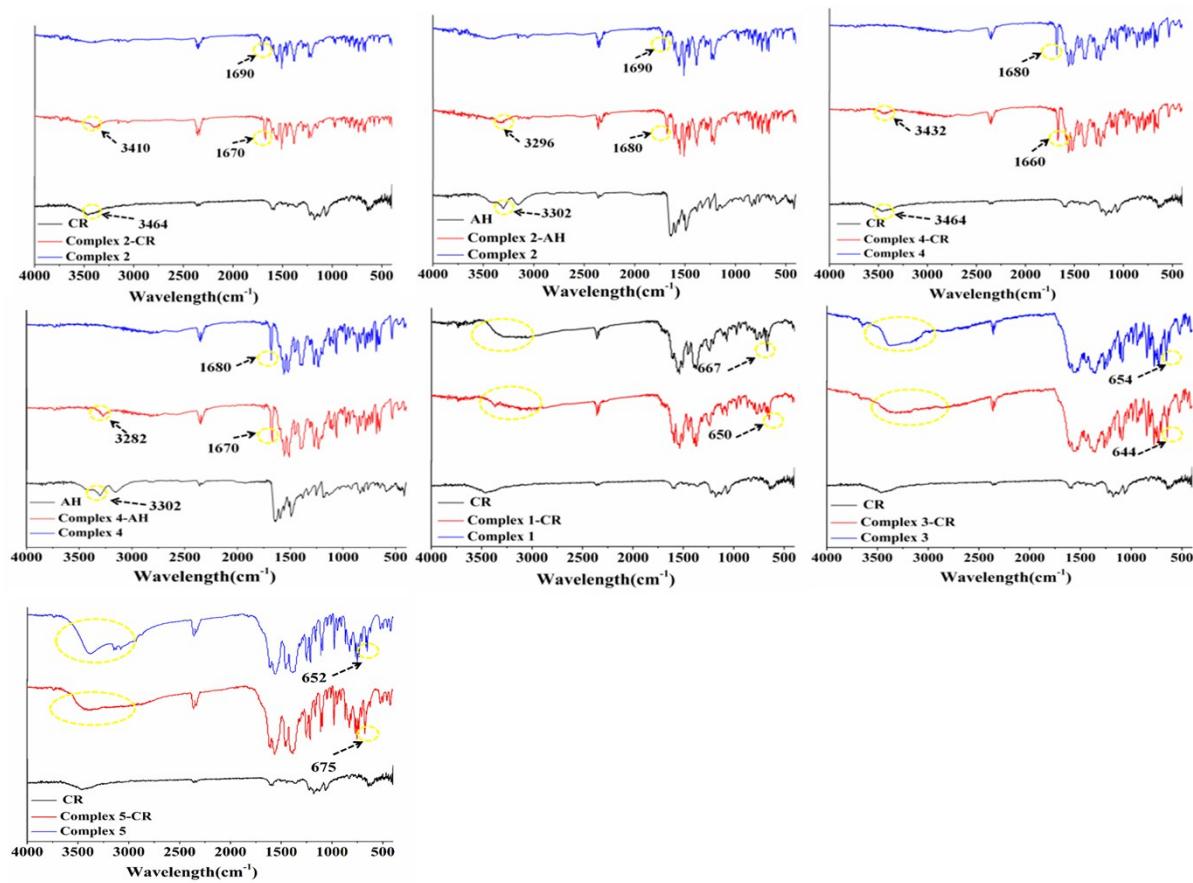


Fig. S21. IR spectra of MOFs **1–5** before and after the adsorption of organic dyes.

Notes and Reference

1. (a) V. A. Blatov, A. P. Shevchenko and D. M. Proserpio, Cryst. Growth Des., 2014, 14, 3576; (b) V. A. Blatov, M. O'Keeffe and D. M. Proserpio, CrystEngComm, 2010, 12, 44; (c) V. A. Blatov, A. P. Shevchenko and V. N. Serezhkin, TOPOS3.2: a new version of the program package for multipurpose crystal-chemical analysis. J. Appl. Crystallogr., 2000, 33, 1193; (d) V. A. Blatov, IUCr CompComm Newsletter, 2006, 7, 4; (e) O. D. Friedrichs, Program SYSTRE 1.14 beta.
2. G. M. Sheldrick, SHELXTL NT, version 5.1, Program for Solution and Refinement of Crystal Structures, University of Göttingen, Göttingen, Germany, 1997.
3. Bruker 2000, SMART, version 5.0, SAINT-plus version 6, SHELXTL, version 6.1, and SADABS version 2.03, Bruker AXS Inc., Madison, WI.
4. (a) Z. Q. Liu, Y. Zhao, P. Wang, Y. S. Kang, M. Azam, S. I. Al-Resayes, X. H. Liu, Q. Y. Lua and W. Y. Sun, Dalton Trans., 2017, 46, 9022; (b) Z. A. Zong, C. F. Bi, Z. Zhu, C. B. Fan, X. M. Meng, X. Zhang and Y. H. Fan, New J. Chem., 2018, 42, 8905; (c) F. Wang, X. H. Ke, J. B. Zhao, K. J.

Deng, X. K. Leng, Z. F. Tian, L. L. Wen and D. F. Li, Dalton Trans., 2011, 40, 11856; (d) A. L. Spek and A. Crystallogr. Sect. A: Fundam. Crystallogr., 1990, 46, 194; (e) A. L. Spek, PLATON, A Multipurpose Crystallographic Tool, Utrecht University, Utrecht, The Netherlands, 2005, or A. L. Spek, J. Appl. Crystallogr., 2003, 36, 7.

5. A. L. Spek, Implemented as the PLATON Procedure, a Multipurpose Crystallographic Tool, Utrecht University, Utrecht, The Netherlands 1998.